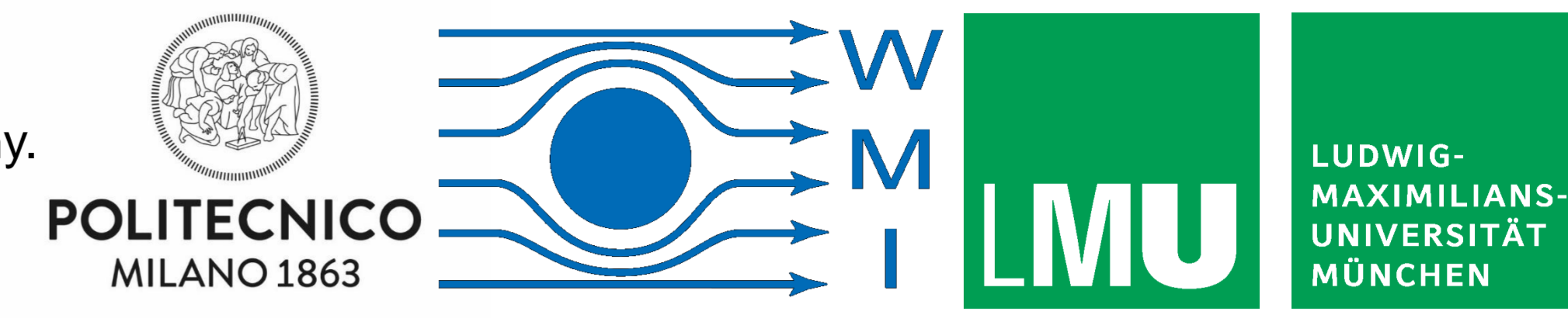


Simulation of tissue dependent magnetic field susceptibility effects in MRI guided radiotherapy

Clarissa KROLL¹, Matthias Opel², Chiara Paganelli³, Florian Kamp⁴, Sebastian Neppi⁴, Guido Baroni³, Olaf Dietrich⁵, Claus Belka⁴, Katia Parodi¹, Marco Riboldi¹

¹Ludwig-Maximilians-Universität LMU, Medical Physics, Garching, Germany, ²Bayerische Akademie der Wissenschaften, Walther-Meißner-Institut, Garching, Germany, ³Politecnico di Milano, Dipartimento di Elettronica- Informazione e Bioingegneria, Milano, Italy, ⁴Ludwig-Maximilians-Universität München, Department of Radiation Oncology, Munich, Germany, ⁵Ludwig-Maximilians-Universität München, Department of Radiology, Munich, Germany.



Motivation

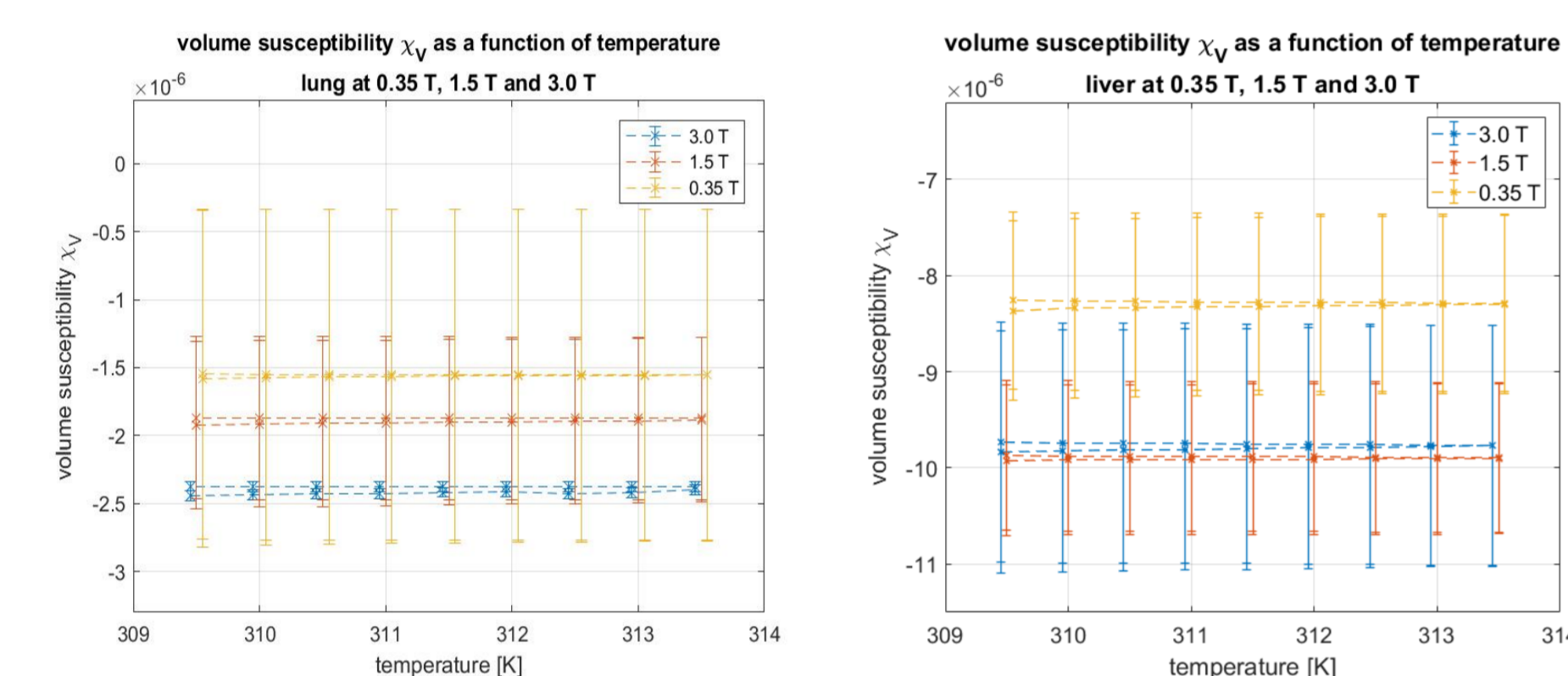
The use of MRI for guidance in external beam radiotherapy must face the issue of spatial distortions, which may hinder accurate geometrical characterization. In this contribution, susceptibility values χ_V for different tissue types were measured, and tissue dependent effects simulated in a digital anthropomorphic CT/MRI phantom.

Susceptibility measurements (SQUID)

SQUID measurements of tissue volume susceptibilities (χ_V in SI units) at 1 bar and a physiological temperature range (309.5 K – 313.5 K).

χ_V are:

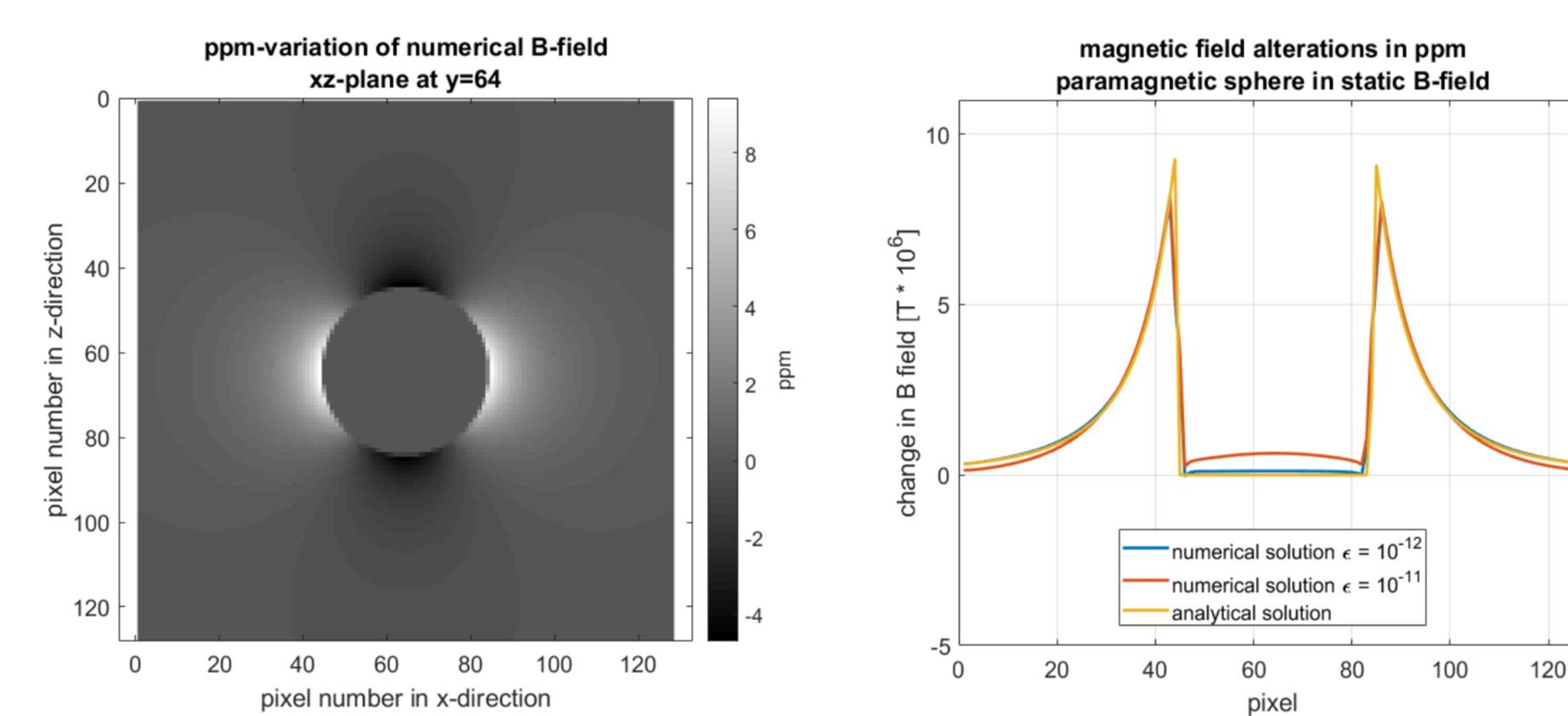
- mainly temperature independent
- subject to high intra-tissue variability
- without clear dependence on magnetic field strength (exception: lung with ferromagnetic hysteresis/ordering)



mean and standard deviation	liver	lung	muscle
$\chi_{V,0.35 T} \cdot 10^6$	-8.32 ± 0.03	-1.69 ± 0.01	-12.7 ± 0.2
$\chi_{V,1.5 T} \cdot 10^6$	-9.91 ± 0.02	-2.06 ± 0.02	-12.84 ± 0.08
$\chi_{V,3.0 T} \cdot 10^6$	-9.80 ± 0.03	-2.63 ± 0.02	-11.9 ± 0.2

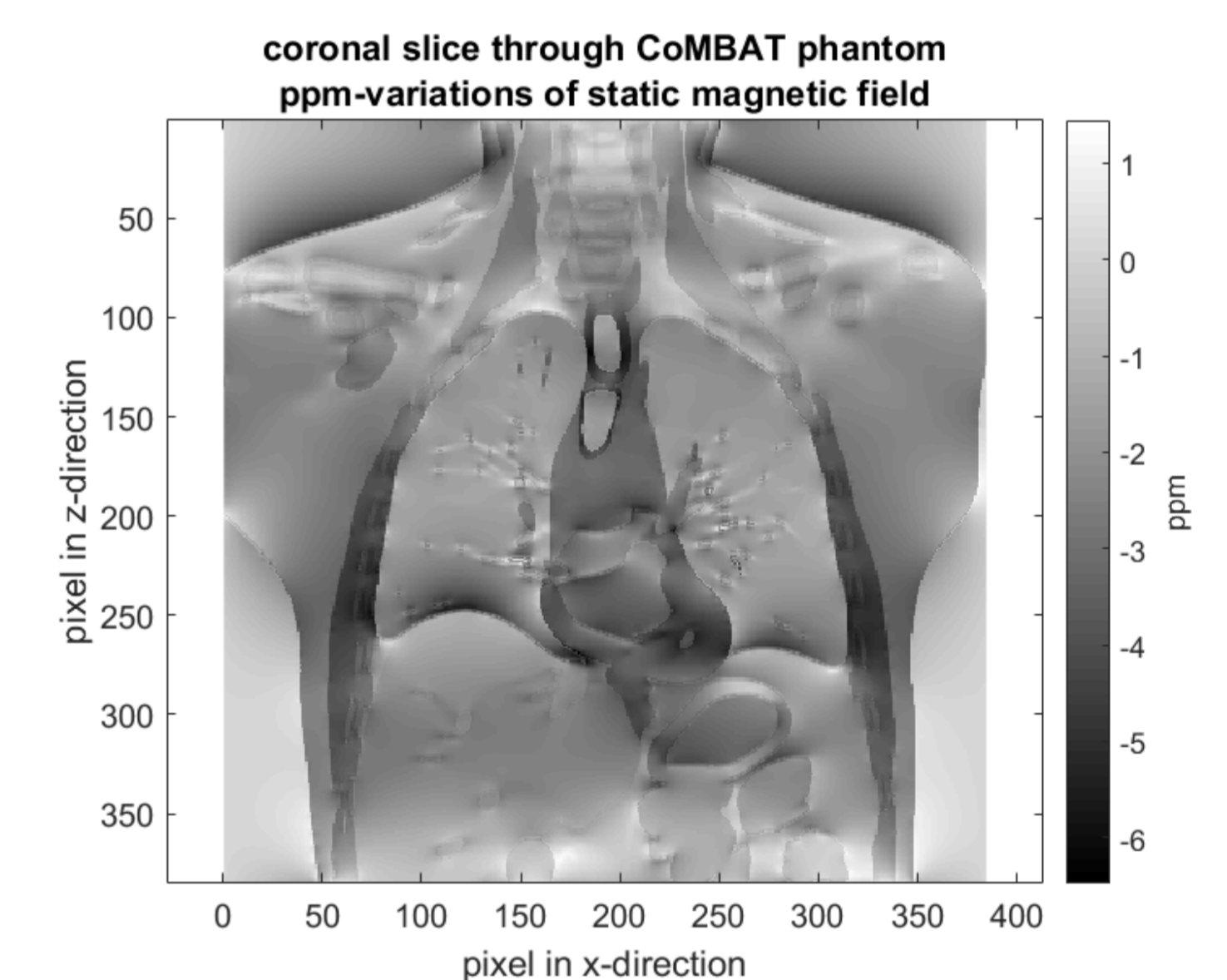
Simulation of susceptibility induced magnetic field changes

- Susceptibility caused magnetic field alterations are determined by iteratively solving the Laplace equation $\nabla(\mu \nabla \Phi_M) = 0^{1,2}$.
- Validation with well known geometries.
- RMS error between analytical and numerical solutions at a 10^{-12} convergence tolerance: ≤ 0.35 ppm, guaranteed accuracy of B_0 in MRI scanner ≤ 1 ppm.
- Results for a paramagnetic sphere:



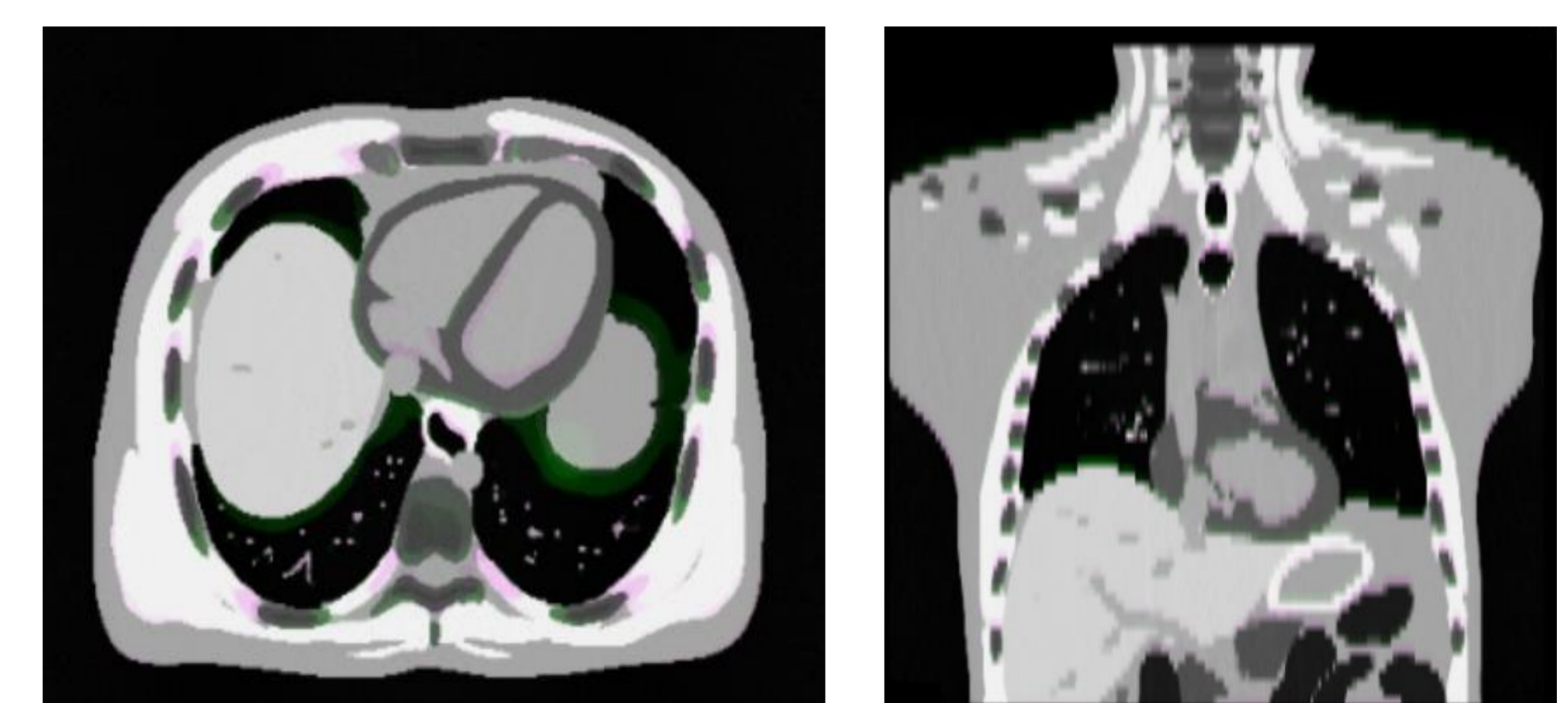
Tissue dependent effects in thorax phantom

- Simulation of susceptibility effects using the determined susceptibilities and literature values^{4,5} for bone, blood, fat, water and air.
- The ppm-differences range from 7.68 ppm to 4.36 ppm at 1.5 T, corresponding to 1.15 mm maximal distortion at a gradient strength of $10 \frac{mT}{m}$.
- Relatively constant magnetic field changes within the same tissues, peaks at tissue boundaries:



Implementation in program for MRI guidance simulation (CoMBAT)

- The CoMBAT program³ can be used to simulate a MR image acquisition for a human thorax model.
- The calculated B-field alterations are translated into a deformation field using the gradient in the direction of the static magnetic field. This allows a quantification of the expected deformation levels in areas of interest.
- The MR images created with the CoMBAT program³ are warped with the deformation fields.
- An overlay of distorted and undistorted MR image allows a visualization of the susceptibility effects on image accuracy.



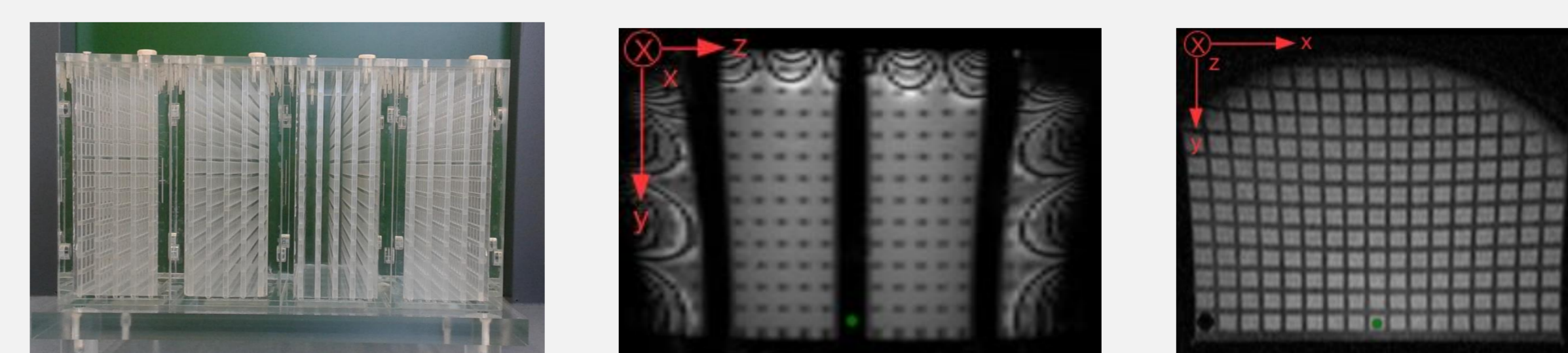
Overlay of undistorted and distorted simulated MR image of the thorax phantom. Areas of agreement are shown in grayscale, areas of disagreement are highlighted in green and pink. Left: axial cut, right: coronal cut.

Conclusion

1. Susceptibility effects can be larger than B_0 effects.
2. The previous approximation of body tissue χ_V with the χ_V of water underestimates the χ_V induced distortions, especially pronounced at tissue boundaries. MRI guidance relies on the tracking of affected regions (e.g. the lung diaphragm).
3. The χ_V of body tissues differ substantially. Through the determination of χ_V for different tissue types, a more realistic representation of distortions and error estimation is feasible.

Outlook

A phantom study dealing with magnetic field alterations due to static field inhomogeneities and gradient nonlinearities is currently ongoing. It will allow a comprehensive simulation of all major effects in spatial distortion for MRI guidance.



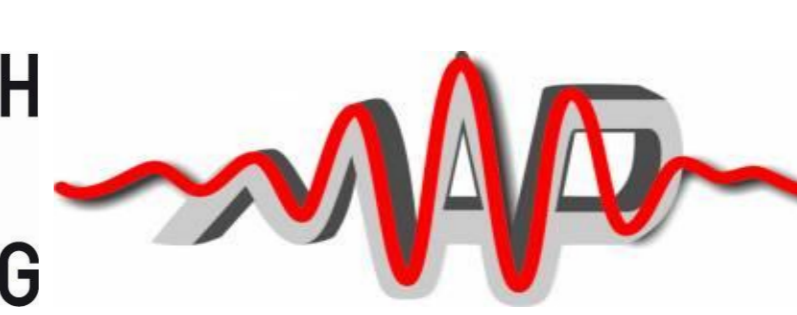
Left: distortion phantom used for MR image acquisition, center: sagittal slice for MR image (TrueFisp sequence), right: axial slice (FLASH sequence)

References

[1] Bhagwandien et al 1992 Numerical analysis of the magnetic field for arbitrary magnetic susceptibility distributions in 2D, Magnetic Resonance Imaging **10(2)** 299-313, doi: 10.1016/0730-725X(92)90489-M; [2] Truong et al 2002 Three-dimensional numerical simulations of susceptibility-induced magnetic field inhomogeneities in the human head Magnetic resonance imaging **20(10)** 759-770, doi: 10.1016/S0730-725X(02)00601-X; [3] Paganelli et al 2017 A tool for validating MRI-guided strategies: a digital breathing CT/MRI phantom of the abdominal site Med Biol Eng Comput. **55(11)** 2001-2014, doi: 10.1007/s11517-017-1646-6; [4] Stanescu et al 2012 Characterization of tissue magnetic susceptibility-induced distortions for MRIGRT Medical Physics **39(12)** 7185-7193, doi: 10.1118/1.4764481; [5] Schenck 1996 The role of magnetic susceptibility in magnetic resonance imaging: MRI magnetic compatibility of the first and second kinds Medical Physics **23(6)** 815-850, doi: 10.1118/1.597854

Acknowledgements

HEINRICH BÖLL STIFTUNG



This research was supported by the Heinrich Böll Foundation and the Munich-Centre for Advanced Photonics (MAP)

PO-1004

Physics track: Imaging acquisition and processing

Clarissa Kroll

DOI: 10.3252/ps.o.eu.ESTRO38.2019

Poster presented at:



Poster SessionOnline.com